Development of a Microfluidic Based Electrochemical Cell for Analyzing Bacterial Biofilms

Ian M. Claydon[*1,2,4], James N. Turner[2,4], Claudia Marques[3,4], David Davies[3,4] and Bahgat G. Sammakia[1,2]
[1] Binghamton University – Department of Mechanical Engineering
[2] Binghamton University – Small Scale Systems Integration and Packaging Center
[3] Binghamton University – Biology Department
[4] Binghamton University – Binghamton Biofilm Research Center
*Corresponding author: Binghamton University, CEA 2115, Binghamton NY 13903, ICLAYDO1@BINGHAMTON.EDU

Abstract: The ubiquitous nature of biofilms has led to a growing need to be able to detect, control, and maintain or remove them. Therefore, a robust testing platform that allows for multiple analytical techniques is required to better understand their multitude of properties is needed. To this end, we have developed a microfluidic-based self-contained electrochemical cell to characterize the biofilm using electrical impedance spectroscopy (EIS). In addition to the EIS capabilities the device is designed to be optically clear to utilize the traditional techniques used in biology while having a removable ceiling that allows access for mechanical probing techniques. This will allow the complex impedance of the biofilm to be quantified and correlated to both its optical and mechanical properties as a function of its stage of development. The development of the electrochemical cell portion of the analysis system is discussed in this paper. The integration of the EIS electrodes requires that the reference and counter remain free of bacteria to maintain accuracy. This paper details the use of COMSOL to determine the optimum geometry and flow conditions for maintaining the sterility of the reference and counter electrodes.

Keywords: Biofilms, Microfluidics, Electrochemical Impedance Spectroscopy.

1. Introduction

Biofilms are surface adhered bacterial cells secured inside of a matrix of extracellular polymeric substance(EPS) [1,2]. The ubiquitous nature of biofilms has led to them being an important field of study due to their prevalence in industrial applications where contamination, biofouling and biocorrosion can occur [3]; a better understanding of them is also relevant to medical fields where biofilms are a cause of persistent infections [4]. The mechanical properties of the EPS matrix are the primary factor in determining biofilm stability and viability and have been shown to be dependent on both the stage of development [4] and the environmental conditions [5,6]. Therefore, measurements of the mechanical properties of the biofilm when coupled with nondestructive measurement technique that can sense initial colonization and track the biofilm's stage of development would be beneficial to numerous industries. The mechanical properties of biofilms were previously studied by Mosier et al. who utilized a microfluidic chamber to culture *Pseudomonas aeruginosa* biofilms for interrogation using an atomic force microscope. While Zheng et al. [7] showed that the stage of maturation of *P. aeruginosa* biofilms could be determined by EIS techniques. These two indicated that a fully self-contained electrochemical cell that was capable of utilizing atomic force microscopy(AFM) and traditional biological investigative techniques would provide a platform to enhance our understanding of biofilms. In order to perform EIS typically three electrodes are required; a working, counter, and reference. To take accurate impedance measurements the reference and counter electrodes must be kept sterile, while the biofilm grows primarily on the working electrode. Multiple unique techniques to maintain the sterility of the reference electrode have been previously reported. The first utilized a salt bridge to prevent the migration of bacteria to the reference electrode [8]. Other methods include the removal and cleaning of the reference electrode prior to measurement [7] and the introduction off the reference electrode upstream from the working electrodes to prevent bacterial growth [9]. An extensive multiphysics modeling study was undertaken in order to develop a microfluidic flow cell that was capable of maintaining the sterility of the reference and counter electrodes while allowing the electrodes

to remain inside of the measurement chamber to prevent environmental contamination. Discussions on the usage of the COMSOL model to determine the potential range of bacteria colonization are contained in the following sections.

2. Use of COMSOL Multiphysics® Software

A three dimensional multiphysics model was developed in order to determine the flow and geometric conditions which would provide a controlled region of reproducible biofilm colonization and development. The baseline geometry for the flow cell was taken from Mosier et al. in their study of *P. aeruginosa*[10] and modified based on the extensive work by Whitesides et al. on microfluidic mixing[11,12] and by Huh et al. on sheath flow[13]. The flow cell, shown in Figure 1, was developed to create a sheath flow in the central measurement chamber in order to limit bacterial proliferation to the region that contains the working electrodes.

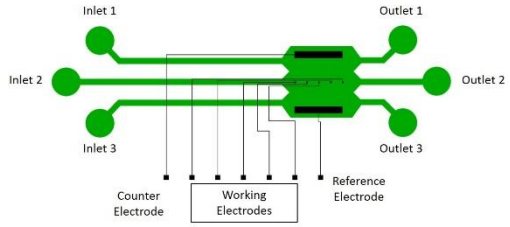

Figure 1. Layout of the complete microfluidic flow cell.

2.1 Numerical Model - Geometry

The overall device design was pared down to the three dimensional model geometry shown in Figure 2 in order to minimize the computational time. This geometry was parametrically generated in order to study the effect of a variety of parameters which are shown in Table 2.

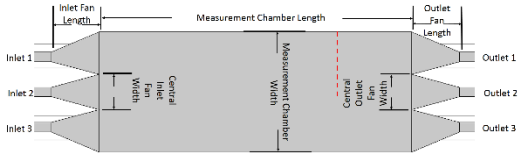

Figure 2. Model used to determine geometric and flow conditions for prevention of bacteria migration within the chamber. Bacteria diffusion characteristics are presented from the location shown by the dashed red line.

2.2 Numerical Model – Physics & Boundary Conditions

In order to model the diffusion of *P. aeruginosa* within the measurement chamber both the Laminar Flow and Transport of Diluted Species physics packages were utilized. The Laminar Flow package, which contains the Navier-Stokes and continuity equations,

$$\rho(\boldsymbol{u}\cdot\nabla)\boldsymbol{u} = \nabla\cdot[-p\boldsymbol{I} + \mu(\nabla\boldsymbol{u} + (\nabla\boldsymbol{u})^T)] + \boldsymbol{F}$$
$$\rho\nabla\cdot(\boldsymbol{u}) = 0$$

was used to determine the velocity of the fluid throughout the flow cell. The Transport of Diluted Species solver, which contains the equations governing diffusion,

$$\nabla\cdot(-D_i\nabla c_i) + \boldsymbol{u}\nabla c_i = R_i$$
$$\boldsymbol{N_i} = -D_i\nabla c_i + \boldsymbol{u}c_i$$

was used to determine the distance the bacteria diffused laterally while being moved through the measurement chamber by convection. All Inlets and Outlets were located on the faces perpendicular to the page with all remaining surfaces being treated as a No Slip, No Flux walls. All three outlets were given Outflow boundary conditions to allow the bacteria to leave the chamber. The built-in material model for water was used for both physics packages while the diffusion rate, shown in Table 2, was set at chosen based on the work by Tran et al.[14]. The diffusion rate utilized is an order of magnitude higher than the reported value for motile *P. aeruginosa* to provide a factor of safety when dealing with other bacteria due to the lack of published data on other species.

2.3 Numerical Model – Geometry Variation Results and Analysis

A set of time independent solutions was obtained from the parametric model using the stationary solver. The results were utilized to determine the maximum dispersion range of the bacteria within the chamber and are presented here. The results of the parametric study are shown in Figure 7 and were taken from the modeling results at the location shown in Figure 2. This location corresponds to the region of electrochemical components furthest from the central inlet which introduces the bacteria and are therefore at the greatest risk of contamination. Figure 7 contains the variations within different sets of parameters for the 7.5mm wide measurement chamber. The 7.5mm wide chamber was chosen to present the results since it showed the greatest variations in response to the variation of the parameters under study. These results show that even over the wide range of parameters studied the distribution of bacteria due to diffusion varies by a practically negligible amount. Therefore, the device was redesigned to have three inlets with individual fan-outs to help prevent bubble nucleation and a single outlet that gently necks down to a single port. This device, shown in Figure 3, was modeled under the same conditions except for the combination of the three outlets into a single channel. The model utilized both the previously modeled diffusion rate and the published diffusion rate. The results from this model are compared to the experimental results in the following sections.

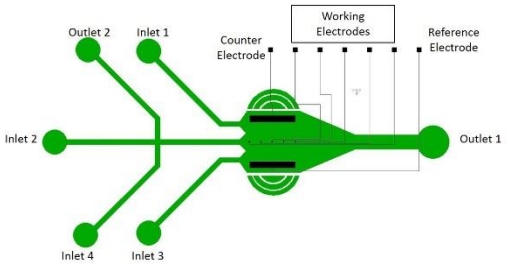

Figure 3. Modified design for experimental verification. The Inlet 4 – Outlet 2 pair was used to introduce the bacteria into the device without risking clogging of the Inlet 2 feed channel.

2.4 Numerical Model – Bacterial Adhesion Study

The second critical aspect of the design was to determine flow conditions that promoted the attachment of P. Aeruginosa to the measurement surface in order to generate a biofilm structure while maintaining the sterile conditions discussed in previous sections. The ability of *P. Aeruginosa PAO1 gfp::GM* to attach to a surface within a moving fluid is highly dependent on its ability to penetrate the boundary layer and make contact with the surface. A model representative of the geometry shown in Figure 3 was generated and is shown in Figure 4. This model was analyzed in a parametric study on the effect of the ratio of flow rates between the sheath flow and the bacteria laden flow with the studied parameters shown in Table 1.

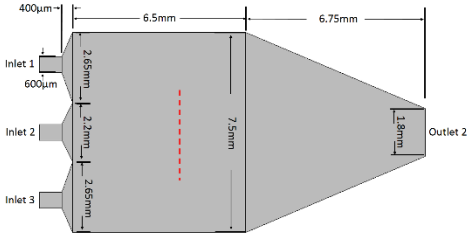

Figure 4. Model to study flow characteristics to increase bacterial adhesion. The thickness of the model is 100µm, and the centers of Inlet 1/3 are located 2.55mm from the center of the measurement chamber. The dashed red line shows the analysis region.

Table 1. Bacterial Adhesion Study Parameters

Nominal Flow Rate	Central Inlet Modification Factors	Sheath Inlets Modification Factors
3.48µl/min	0.1, 0.25, 0.5, 0.75, 1	0.1, 0.25, 0.75, 1, 2

The modeling results are presented in Figure 5 with a portion of the results omitted for clarity. The results show the expected trend of decreasing the width of the diffusion band by increasing the ratio of the sheath flow to the center flow. The result also shows the effect that the various ratios have on the velocity in the region. From these results flow rates of 0.34µl/min and 2.61µl/min were chosen for the central and sheath inlets respectively. These flow rates were used in seeding the chamber with bacteria.

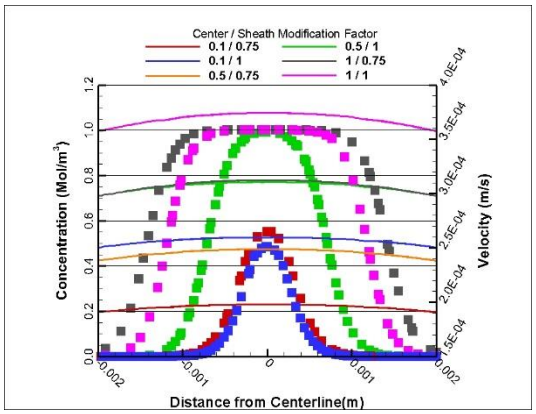

Figure 5. Effect of the variation of inlet flow rates on the velocity and diffusion characteristics in the center portion of the flow cell. The squares show the concentration of bacteria and the lines show the velocity. Both are with respect to the distance from the centerline of the reactor.

3. Experimental Results

With the modeling results as a guide, a polydimethylsiloxane (PDMS) (Dow Corning) replica of the geometry shown in Figure 3 was created. Using an oxygen plasma the PDMS portion of the flow cell was bonded to an Eagle Glass(Corning) microscope slide. In order to guarantee sterility of the system prior to inoculation, the microfluidic portions of the system were sterilized using a bleach based solution, while the Tygon tubing(Saint-Gobain) that is used to connect the syringes on the syringe pumps to the chamber were autoclaved. A set of four 10ml syringes (BD Scientific) used to drive the flow through the device were sterilized by the manufacturer. The syringes were opened, filled and stored in the sterile environment of a SterilGARD III Advance(The Baker Company) hood. Three of the syringes were filled with sterile mixture of Lysogeny broth and gentamicin while the fourth syringe was filled with an incubated overnight culture of *P. Aeruginosa PAO1 gfp::GM* in Lysogeny broth and gentamicin. The final assembly of the sterile components took place inside the hood to prevent contamination of the device. The three syringes containing sterile media were connected to Inlets 1/2/3 while the syringe containing the *P. Aeruginosa* solution was connected to Inlet 4 (Figure 3).

Using two Legato 270(KD Scientific) syringe pumps to control the flow the microfluidic connections were purged of air using Outlet 2 (Figure 3), in order to prevent contamination of the flow cell. This was performed by clamping the tubing coming from Outlet 1 to force the flow through Outlet 2, sequencing the pumps to fill the measurement chamber with sterile fluid, remove trapped air, and pressurize the measurement chamber of the system. With the measurement chamber and all sterile lines pressurized the pump connected to Inlet 4 was cycled to purge the air out through Outlet 2. This technique prevented the bacteria from prematurely entering the measurement chamber. Once the gas was purged from the system the syringes connected to Inlet 1 and Inlet 3, which form the sheath flow each were set to a constant flow rate of 2.61µl/min. At this point the tubing connected to Outlet 2 was clamped to prevent flow through it and the clamp on Outlet 1 was removed. After the clamp was removed the second pump, which contained the syringe inoculated with *P. Aeruginosa PAO1 gfp::GM* was set to a constant flow rate of 0.34µl/min. These conditions were maintained for period of twenty hours at which point the flow was stopped and the dispersion of bacteria was analyzed with a fluorescent microscope. The preliminary results, shown in Figure 6, show the diffusion of *P. Aeruginosa PAO1 gfp::GM* which is marked by a pair of green lines. The darker regions between the two lines were confirmed to be *P. Aeruginosa PAO1 gfp::GM* through the excitation of their fluorescence. The lack of a fluorescence response above and below the marked region showed that over the time frame studied there was no proliferation of bacteria into this region. These results show that the settlement and growth of *P. Aeruginosa PAO1 gfp::GM* can be controlled by a sheath flow and are inhibited from reaching the locations of the reference and counter electrodes. The cause of the asymmetry of the diffusion in Figure 6 was a piece of debris trapped within the flow cell from the autoclaving process.

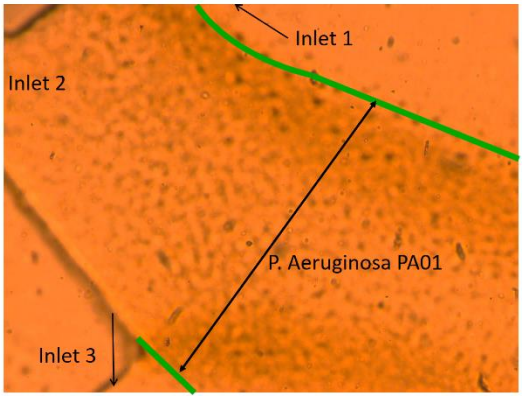

Figure 6 Diffusion of P. Aeruginosa PAO1 within the measurement chamber is limited by the sheath flow.

5. Conclusions

Through the use of the COMSOL Multiphysics® software packages a microfluidic based electrochemical cell was developed for use in the analysis of biofilms. In the model *P. aeruginosa* was modeled as a dilute chemical species to determine both the flow conditions that would prevent the bacteria from colonizing the reference and counter electrodes of the electrochemical cell, and a range of conditions that would allow the bacteria to colonize the measurement surfaces. The models were experimentally investigated with the initial results providing confidence that the modeling results can be replicated in an actual device. Further investigation of the accuracy of the modeling effort is planned.

6. References

1. Klapper, I., Rupp, C. J., Cargo, R., Purvedorj, B., and Stoodley, P., "Viscoelastic fluid description of bacterial biofilm material properties," Biotechnol. Bioeng., **80**, pp. 289–296 (2002)
2. Rupp, C. J., Fux, C. A., and Stoodley, P., "Viscoelasticity of Staphylococcus aureus Biofilms in Response to Fluid Shear Allows Resistance to Detachment and Facilitates Rolling Migration," Appl. Environ. Microbiol., **71**, pp. 2175–2178 (2005)
3. Coetser, S. E., and Cloete, T. E., "Biofouling and Biocorrosion in Industrial Water Systems," Critical Reviews in Microbiology, **31**, pp. 213–232 (2005)
4. Costerton, J. W., Stewart, P. S., and Greenberg, E. P., "Bacterial biofilms: a common cause of persistent infections," Science, **284**, pp. 1318–1322 (1999)
5. Isberg, R. R., and Barnes, P., "Dancing with the Host: Flow-Dependent Bacterial Adhesion," Cell, **110**, pp. 1–4 (2002)
6. Purevdorj, B., Costerton, J. W., and Stoodley, P., "Influence of Hydrodynamics and Cell Signaling on the Structure and Behavior of Pseudomonas aeruginosa Biofilms," Appl. Environ. Microbiol., **68**, pp. 4457–4464 (2002)
7. Zheng, L. Y., Congdon, R. B., Sadik, O. A., Marques, C. N. H., Davies, D. G., Sammakia, B. G., Lesperance, L. M., and Turner, J. N., "Electrochemical measurements of biofilm development using polypyrrole enhanced flexible sensors," Sensors and Actuators B: Chemical, **182**, pp. 725–732 (2013)
8. Bayoudh, S., Othmane, A., Ponsonnet, L., and Ben Ouada, H., "Electrical detection and characterization of bacterial adhesion using electrochemical impedance spectroscopy-based flow chamber," Colloids and Surfaces A: Physicochemical and Engineering Aspects, **318**, pp. 291–300 (2008)
9. Ben-Yoav, H., Freeman, A., Sternheim, M., and Shacham-Diamand, Y., "An electrochemical impedance model for integrated bacterial biofilms," Electrochimica Acta, **56**, pp. 7780–7786 (2011)
10. Mosier, A. P., Kaloyeros, A. E., and Cady, N. C., "A novel microfluidic device for the in situ optical and mechanical analysis of bacterial biofilms," Journal of Microbiological Methods, **91**, pp. 198–204 (2012)
11. Whitesides, G. M., "The origins and the future of microfluidics," Nature, **442**, pp. 368–373. (2006)
12. Dertinger, S. K. W., Chiu, D. T., Jeon, N. L., and Whitesides, G. M., "Generation of Gradients Having Complex Shapes Using Microfluidic Networks," Analytical Chemistry, **73**, pp. 1240–1246. (2001)
13. Huh, D., Gu, W., Kamotani, Y., Grotberg, J. B., and Takayama, S., "Microfluidics for flow cytometric analysis of cells and particles," Physiol. Meas., **26**, p. R73 (2005)
14. Tran, V. B., Fleiszig, S. M. J., Evans, D. J., and Radke, C. J., "Dynamics of Flagellum- and

Pilus-Mediated Association of Pseudomonas aeruginosa with Contact Lens Surfaces," Applied and Environmental Microbiology, **77**, pp. 3644–3652 (2011)

7. Acknowledgements

Thank you to Elin Mina, Paul Woods and Minyoung Kim for their guidance and advice in all aspects of preparation and conduction of the experiment. Laboratory space and supplies were provided by the Binghamton Biofilm Research Center. Funding for this research was provided by the S3IP NY State Center of Excellence.

11. Appendix

Table 2 Geometry Variation Model Parameters. Note the Diffusion Rate chosen for *P. Aeruginosa* is an order of magnitude higher than the published value to provide a factor of safety.

Model Parameters	2.5mm Wide Measurement Chamber Dimensions	5.0mm Wide Measurement Chamber Dimensions	7.5mm Wide Measurement Chamber Dimensions
Measurement Chamber Length	6.5mm	6.5mm	6.5mm
Flow Cell Depth	100µm	100µm	100µm
Inlet Width	200µm	400µm	600µm
Outlet Width	200µm	400µm	600µm
Diffusion Rate	$1e^{-9}cm^2/sec$	$1e^{-9}cm^2/sec$	$1e^{-9}cm^2/sec$
Inlet Flow Rate	1.16µl/min	2.32µl/min	3.48µl/min
Inflow at Inlet 2	$1mol/m^3$	$1mol/m^3$	$1mol/m^3$
Outlet Conditions	0Pa (Suppress Backflow)	0Pa (Suppress Backflow)	0Pa (Suppress Backflow)
Inlet Fan Length	100µm, 550µm, 1000µm	100µm, 550µm, 1000µm	100µm, 550µm, 1000µm
Central Inlet Fan Width	133µm, 733µm, 1333µm	266µm, 1366µm, 2666µm	400µm, 2200µm, 4000µm
Outlet Fan Length	100µm, 550µm, 1000µm	100µm, 550µm, 1000µm	100µm, 550µm, 1000µm
Central Outlet Fan Width	133µm, 733µm, 1333µm	266µm, 1366µm, 2666µm	400µm, 2200µm, 4000µm

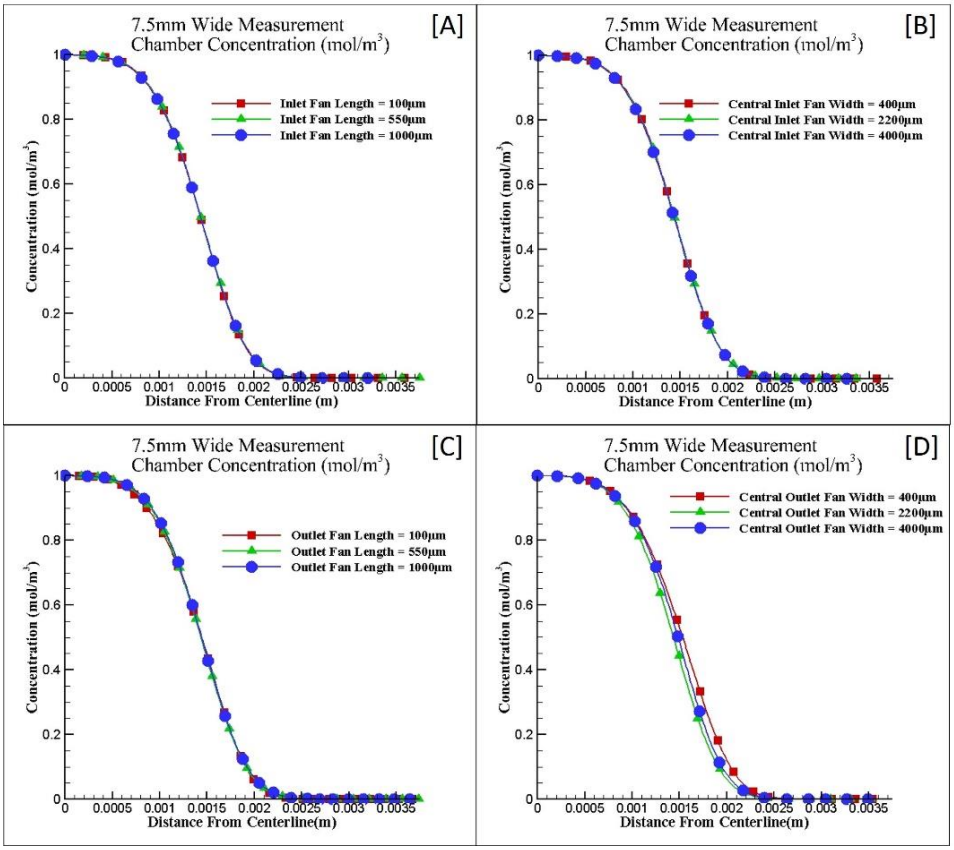

Figure 7 Bacteria concentration results from the geometry variation study. Shown is the variation in the resulting concentration for the variation of [A] Inlet Fan Length, [B] Central Inlet Fan Width, [C} Outlet Fan Length, and [D] Central Outlet Fan Width.